

## Orientation dependence of the ionization of CO and NO in an intense femtosecond two-color laser field

H. Li,<sup>1</sup> D. Ray,<sup>1</sup> S. De,<sup>1</sup> I. Znakovskaya,<sup>2</sup> W. Cao,<sup>1</sup> G. Laurent,<sup>1</sup> Z. Wang,<sup>1</sup> M. F. Kling,<sup>1,2</sup> A. T. Le,<sup>1</sup> and C. L. Cocke<sup>1</sup>

<sup>1</sup>*J.R. Macdonald Laboratory, Department of Physics, Kansas State University, Manhattan, Kansas 66506, USA*

<sup>2</sup>*Max-Planck Institut für Quantenoptik, D-85748 Garching, Germany*

(Received 27 May 2011; published 24 October 2011)

Two-color (800- and 400-nm) short (45-fs) linearly polarized pulses are used to ionize and dissociate CO and NO. The emission of  $C^q+$ ,  $N^q+$ , and  $O^+$  fragments indicates that the higher ionization rate occurs when the peak electric field points from C to O in CO and from N to O in NO. This preferred direction is in agreement with that predicted by Stark-corrected strong-field-approximation calculations.

DOI: [10.1103/PhysRevA.84.043429](https://doi.org/10.1103/PhysRevA.84.043429)

PACS number(s): 34.50.Rk, 33.80.Rv, 42.65.Ky

### I. INTRODUCTION

When intense field pulses are applied to atoms and molecules in the tunneling region the ionization rate can be approximately calculated by quasistatic tunneling theory [1] or other well-known treatments [2–4]. When the system is a diatomic molecule, it is well established that this rate depends on the angle between the internuclear axis and the laser polarization. A convenient treatment of the rate in this case is given by molecular tunneling theory, which predicts an enhanced ionization rate of an orbital [usually the highest occupied molecular orbital (HOMO)] to occur when the molecule is aligned such that the laser polarization lies along the angular maxima of the orbital [5] [the molecular orbital Ammosov-Delone-Krainov (MO-ADK) theory]. Several different experimental approaches have been used to measure the angular dependence of the ionization rate for small molecules, including momentum imaging with linear polarization [6–11], circular polarization [12–14], and impulsive and adiabatic prealignment [15–18].

This result has shown that the shape of the HOMO can be mapped out using the ionization rate [6–11,15–17]. For the case of heteronuclear molecules, the ionization rate is predicted by the MO-ADK theory to be orientation dependent (as opposed to only alignment dependent) and to maximize when the tunneling of the electron occurs in the direction in which the square of the orbital wave function maximizes [8]. Several recent experiments have measured the orientation dependence of the ionization rate [13,14,17–20] for several chosen molecules. This orientation dependence in several cases [13,14] has been attributed not to the shape of the orbits but to the orientation dependence of the effective ionization potential of the HOMO (or HOMO-1) (Stark shifted) of the molecule. This dependence arises because of the dipole energy of the interaction between both the neutral and ionized molecule and the electric field. The effect of including the linear Stark effect alone tends to predict favored ionization for exactly the opposite orientation from that predicted by the MO-ADK theory [21].

The orientation dependence of the ionization rate has recently been studied theoretically by Madsen and co-workers [17,21–24]. Three distinguishable contributors to the orientation dependence have been identified. For small molecules with relatively low polarizabilities, the MO-ADK theory prediction, modified by including the linear Stark shift of the

ionization potential, was found to be adequate. The preferred orientation for favored ionization remains the same as that predicted by the MO-ADK theory, but weakened by the linear Stark effect. For molecules with large polarizabilities, this treatment is inadequate because the electron distribution around the molecule tends to follow the applied field, demanding a more complete treatment. A simple model based on this idea was proposed, which proposes favored ionization of carbonyl sulfide (OCS) for an orientation exactly opposite to that predicted by the MO-ADK theory [17].

In this paper we report the orientation dependence of the strong-field ionization of CO and NO by two-color femtosecond pulses. Both of these molecules lie in the class of small polarizabilities. For both CO and NO we find that enhanced ionization occurs when the molecule is oriented with the electric field pointing toward the O atom, which is the direction expected from the MO-ADK theory alone for the HOMO but opposite that predicted by the Stark shift alone. A similar two-color study on 1-iodohexane has been performed by Ohmura *et al.* [25] and recently we became aware of a similar study by this group [26] on two-color ionization of CO. Our results are in complete agreement with theirs. The present paper supplements that one in reporting some additional data on NO, the kinetic-energy-release (KER) dependence of the asymmetry, and the asymmetry of the detected electrons including rescattered electrons. We note that this work is closely related to, but should not be confused with, recent work on the asymmetry of the charge distribution from homonuclear molecules fragmented by two-color fields [27].

There are two issues that should be separated when discussing the orientation dependence of heteronuclear diatomic molecules: (a) which way the molecule should be oriented in order to maximize the ionization rate and (b) which way the electron preferentially goes. These are quite different questions. If the answer to question (a) is known, then we know which way the electron is preferentially initially extracted, i.e., in the direction opposite to that of the field (the electron has a negative charge); however, this is not the direction in which the electron will finally be detected. Indeed, in a strong-field picture, the final momentum of the electron is given not by the direction in which it tunnels but by the vector potential at the time it does so and, unfortunately, the vector potential is typically passing through zero at the time most electrons are emitted. Thus predicting which way the electrons will end up is very much not intuitive. In a recent two-color study

of Xe [28] we have found that the maximum asymmetry of emission of the direct electrons in a two-color field occurs not for the two-color phase that maximizes the asymmetry of the field but for a phase that is shifted by about  $\pi/2$  relative to this value. Electrons emitted at the maximum field asymmetry have relatively little final asymmetry themselves. In contrast, the backscattered electrons that populate the high-energy part of the plateau behave in a very intuitive way. When the two-color phase is such that the electrons are preferentially extracted to the left, the backscattered electrons will also end up scattered to the left. As described in Ref. [28] and again later in the present paper, this behavior offers a robust way to determine the sign and value of the two-color phase. Furthermore, this effect is found here to be very similar for diatomic molecules and for spherically symmetric Xe. The field dynamics determines the final direction of detection of the electron more than the details of the structure of the emitter.

## II. EXPERIMENT

The experimental arrangement is discussed in Ref. [28]. A two-color (800- and 400-nm) field was created in a collinear geometry using a  $\beta$ -barium-borate (BBO) crystal, a rotatable calcite plate, and a zeroth-order half-wave plate (at 800 nm). The time length of the 800-nm pulse was  $30 \pm 10$  fs; the length of the 400-nm pulse was not measured directly, but is expected to be somewhat longer. The intensity of the 400-nm component was typically  $(10 \pm 3)\%$  of that of the 800-nm field. The relative phase of the two components was adjusted by rotating the calcite plate. This field was focused onto an effusive gas jet of Xe, CO, or NO in a velocity-map-imaging system [18,29,30] and either electrons or ions were detected. The images were Abel inverted using the usual procedure [31]. The energy spectra and asymmetries were generated for those electrons making an angle of less than  $15^\circ$  with respect to the polarization vector.

## III. ASSIGNMENT OF ABSOLUTE TWO-COLOR PHASE

The absolute phase of the two colors was established by measuring the rescattered electrons from Xe. Figure 1 shows the asymmetry of emission of electrons from Xe as a function of the two-color phase  $\phi$ , where the electric field (in the up direction) is given by

$$E(t) = E_1 \cos(\omega t) + E_2 \cos(2\omega t + \phi).$$

The measured asymmetry of Xe electrons [defined as  $(Y_{\text{up}} - Y_{\text{down}})/(Y_{\text{up}} + Y_{\text{down}})$ , where the polarization is in an up-down direction and  $Y$  is the electron yield] is shown in a density plot as a function of  $\phi$  and the electron energy. The rescattered electrons near the maximum backscattering energy [often referred to as the backscattering ridge (BRR) [32] occur near an electron energy of 30–50 eV. It is clear that it is necessary to identify the backscattered electron unambiguously in order to use such a plot to determine the absolute scale of  $\phi$  since the softer electrons have a very different asymmetry profile from the backscattered ones.

Assigning the absolute two-color phase on the basis of the asymmetry plot is somewhat problematic due to the saturation

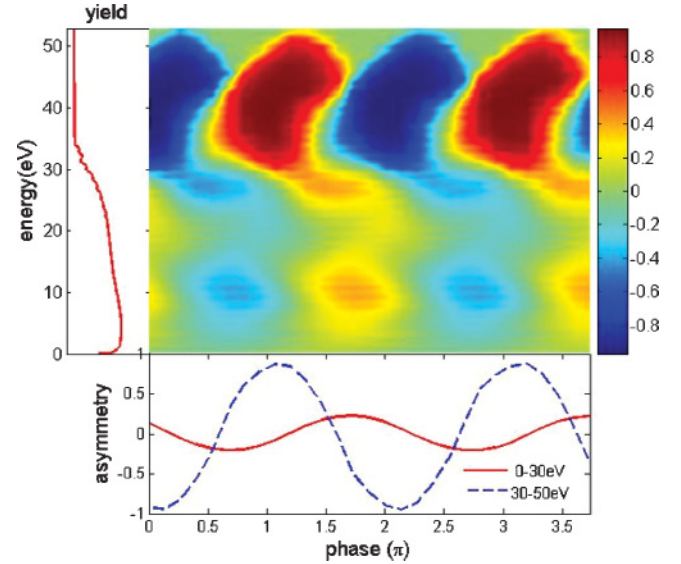


FIG. 1. (Color online) Density plot of the asymmetry of emission of electrons from Xe at an intensity of  $(0.7 \pm 0.1) \times 10^{14}$  W/cm<sup>2</sup> as a function of electron energy and two-color phase  $\phi$ . A projection of the yield versus electron energy is shown on a logarithmic scale in the left panel, while the bottom panel shows plots of asymmetry versus phase for two chosen slices of electron energy.

of the asymmetry over a range in  $\phi$ . Figure 2(a) shows a comparison of the electron yield, rather than the asymmetry, in the down direction as a function of  $\phi$ . By comparing this with the theoretical yield from a solution of the time-dependent Schrödinger equation (TDSE) [28] it is possible to assign the actual absolute phase to Figs. 1 and 2. The hook-shaped pattern, which is characteristic of the BRR electrons [28], is clear in both figures. Indeed, the observation of this structure is almost necessary to be sure that one has located the BRR electrons. As discussed in Ref. [28], the maximum of the rescattered electron energy does not occur quite at  $\phi = 0$  for which the field has its maximum asymmetry but somewhat past

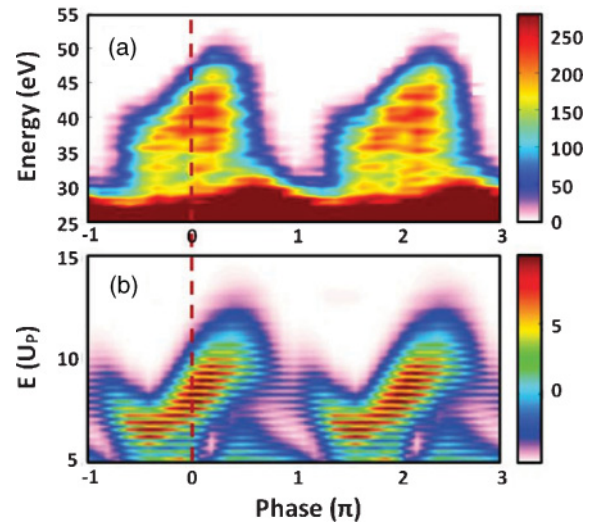


FIG. 2. (Color online) (a) Density plot of down electrons as a function of electron energy and phase. (b) Theoretical TDSE calculation for this process [28].

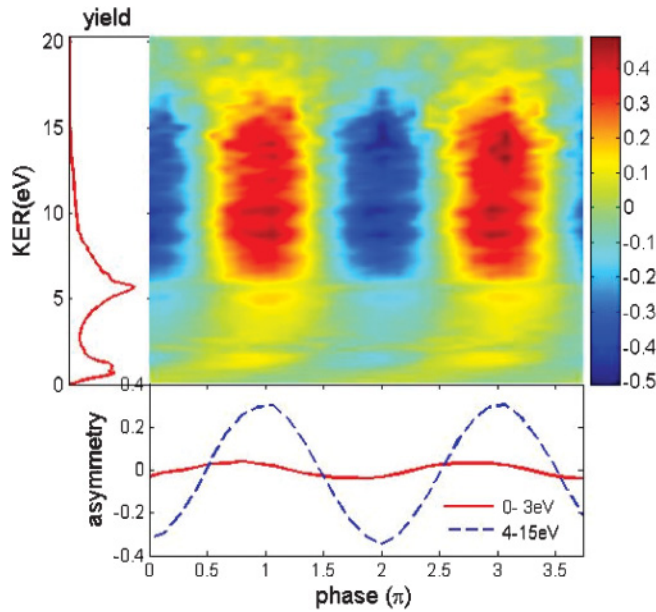


FIG. 3. (Color online) Density plot of the asymmetry of emission of  $C^+$  ions from CO at an intensity of  $2 \times 10^{14} \text{ W/cm}^2$  as a function of two-color phase  $\phi$  and KER. A projection of the yield versus KER is shown in the left panel, while the bottom panel shows plots of asymmetry versus phase for two chosen slices of the KER.

that point. The absolute scale of  $\phi$  in this paper was assigned on the basis of this comparison, with a further check as discussed below. The *in situ* ratio of  $E_2/E_1$  can also be deduced from this figure to be  $0.2 \pm 0.08$ .

## IV. RESULTS

### A. Asymmetry of ion yields

#### 1. CO

Figure 3 shows the  $\phi$  dependence of the up-down asymmetry of emission of  $C^+$  ions as a function of their KER. The groups near 1 and 6–8 eV correspond to dissociation of the CO molecule into  $C^+ + O$  and  $C^+ + O^+$ , respectively. A number of dissociative states are involved in each case, as discussed in Refs. [9–11,33–35]. The asymmetry for the  $C^+ + O^+$  channel shows very little dependence on KER. The asymmetry for the  $C^+ + O$  channel has the same sign and nearly the same phase as the double ionization channel over most of the KER range, with somewhat weaker asymmetries. The consistent sign and phase of the asymmetry supports the supposition that the asymmetry is determined mainly by the removal of the first electron from the CO molecule. Figure 4 further supports this by showing that  $C^{2+}$  ions show the same pattern. Figure 5 shows that the  $O^+$  ions exhibit just the opposite asymmetry, which is again to be expected if the preferred orientation of the molecule in the first step is what determines the asymmetry. Note that the maxima of the asymmetries occur at  $\phi = 0$  and  $\pi$ , as would be expected and confirming the absolute two-color scale assigned above. Effectively, it would have been sufficient to use the backscattered electrons only to assign the sign of the phase scale.

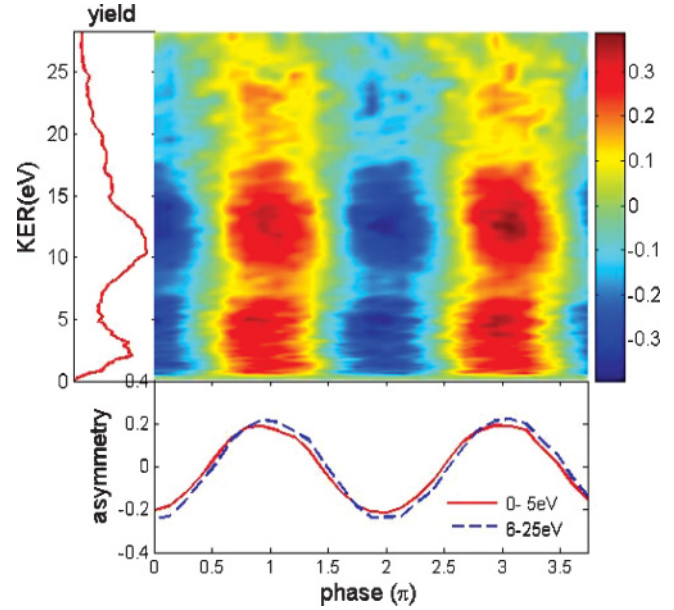


FIG. 4. (Color online) Similar to Fig. 3, but for  $C^{2+}$  ions.

#### 2. NO

Figures 6 and 7 show similar figures for  $N^+$  and  $O^+$  ions from NO. The groups below a KER near 2 eV and above 5 eV correspond to dissociation of the NO molecule into  $N^+ + O$  and  $N^+ + O^+$ , respectively. The asymmetry is clear but weaker than for CO.

### B. Electron distributions

Figures 8 and 9 show electron spectra, similar to those of Figs. 1 and 2, but now for a CO target. The characteristic hook-shaped pattern for the BRR electrons is still visible, although not as distinct as was the case for Xe. The backscattered electrons behave as intuitively expected: Electrons extracted

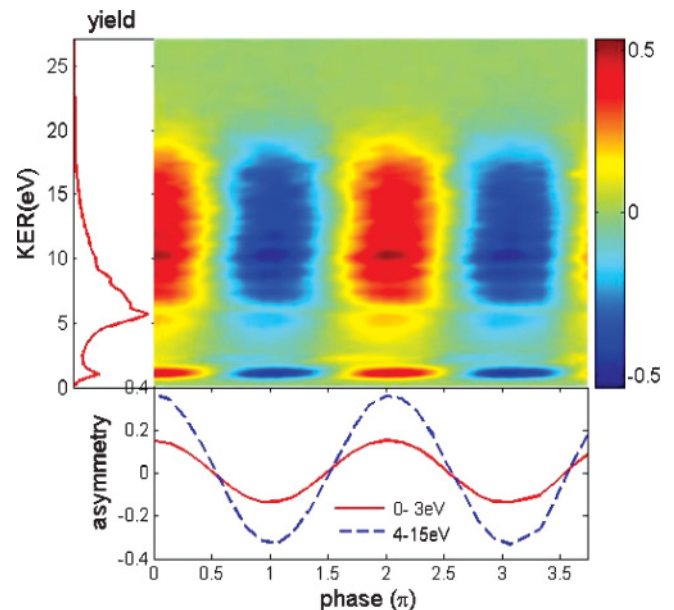


FIG. 5. (Color online) Similar to Fig. 3, but for  $O^+$  ions.

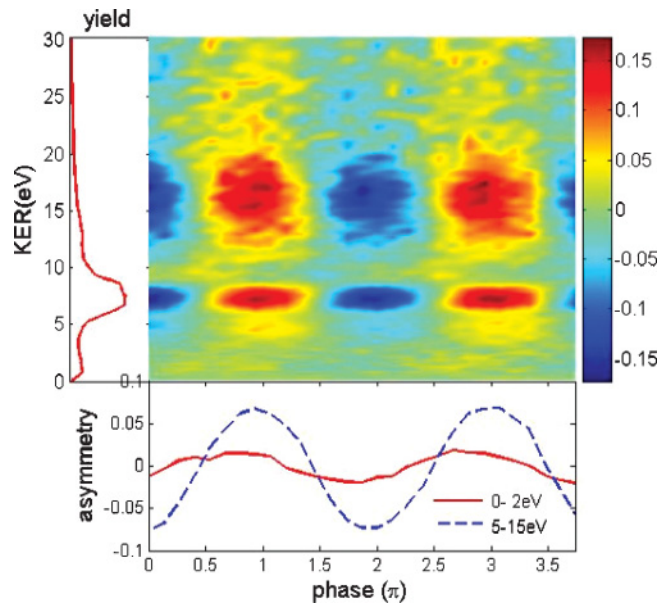


FIG. 6. (Color online) Similar to Fig. 3, but for  $N^+$  from NO at an intensity of  $3 \times 10^{14}$  W/cm<sup>2</sup>.

for  $\phi = 0$ , when the field is up, exit down, rescatter, and finally are observed down. In contrast, the direct electrons for the same field direction end up preferentially being observed up, that is, they leave the CO molecule going in the direction the field pushed them, but eventually reverse direction in the combined action of the molecular potential and the field to be observed in the opposite direction. The similarity of this spectrum to that of Figs. 1 and 2 emphasizes that little is learned about the influence of the CO structure by looking at the asymmetry of the direct electrons. We point out that this is not a coincidence experiment: We have not preselected an orientation of the CO molecule in recording the electron spectrum, although we know from the ion distributions that the ionization rate to some extent does this for  $\phi = 0$  and  $\pi$ .

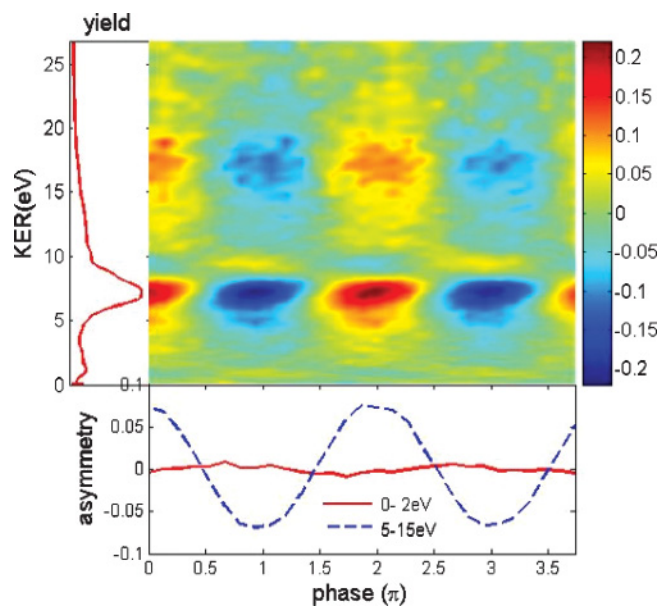


FIG. 7. (Color online) Similar to Fig. 3, but for  $O^+$  ions from NO.

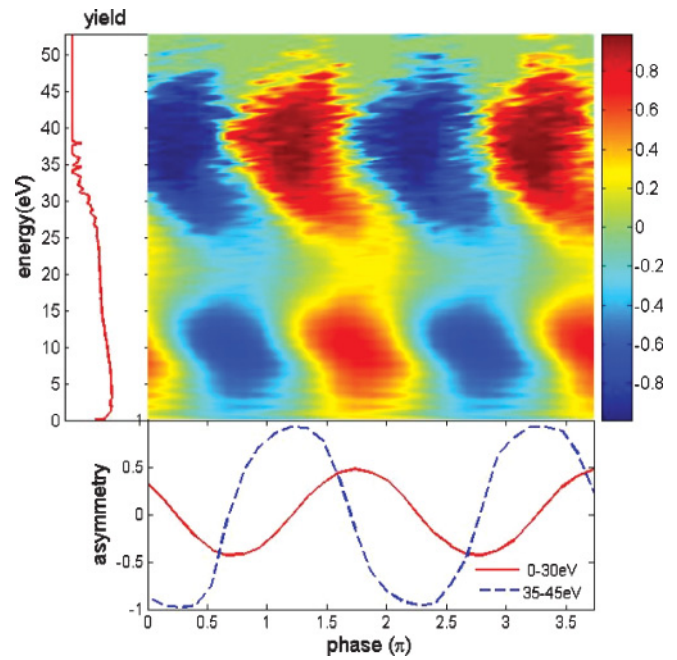


FIG. 8. (Color online) Similar to Fig. 1, but for a CO target.

## V. DISCUSSION

The data show that both molecules ionize more easily when the electric field points toward the O atom, with a much larger asymmetry observed for CO than for NO. Figure 10 shows plots of the HOMO for CO and NO. On the basis of the MO-ADK model one would expect that the HOMO of CO would ionize more easily when the electric field points from the C atom to the O atom [7]. The Stark shift effect would predict preferential ionization for just the opposite direction of the field. The dipole moment of the HOMO points from the C atom to the O atom, which means that when the field is in the same direction the effective binding energy of the electron increases and the tunneling rate should decrease. In fact, both aspects must enter into the problem, and it is not *a priori* obvious which effect will win. This situation was considered in depth by Dimitrovski *et al.* [21], who considered the orientation dependence of ionizing OCS for various approximations. In the same spirit we show in Fig. 11 the dependence of the ionization rate of CO on the angle between the electric field and the molecule, where  $0^\circ$

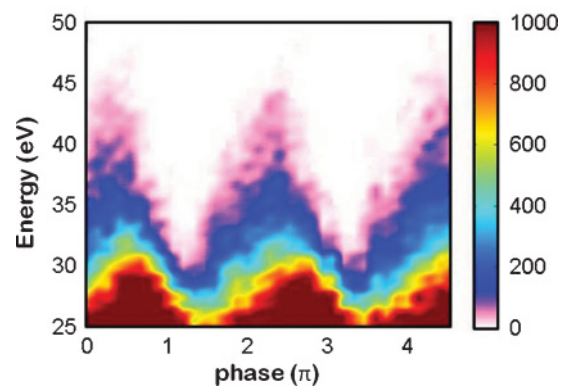


FIG. 9. (Color online) Similar to Fig. 2, but for a CO target.

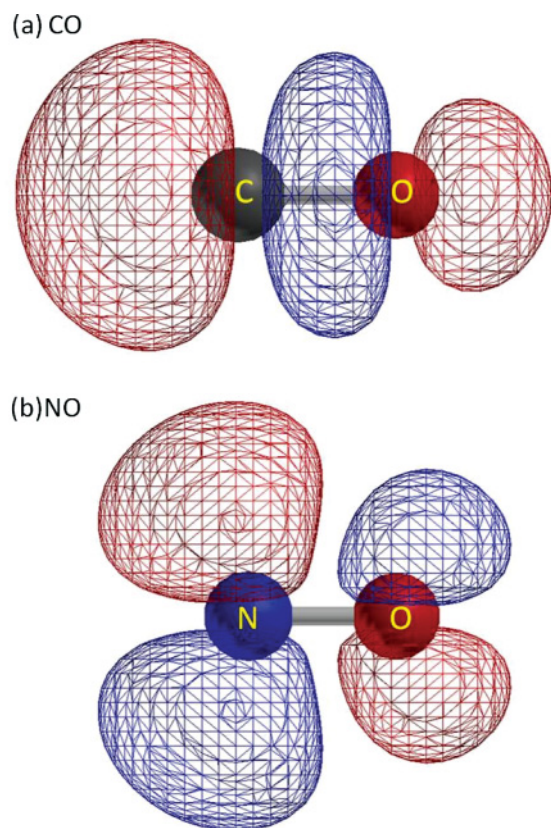


FIG. 10. (Color online) Schematic of the HOMO of (a) CO and (b) NO.

corresponds to the field pointing from the C atom to the O atom. Figure 11(a) shows the MO-ADK theory rate both with and without a Stark correction. Specifically, for the Stark-corrected MO-ADK theory [or strong-field approximation (SFA)] calculations, we keep the standard MO-ADK theory (or SFA) equation but use the Stark-shifted ionization potential. Within the single-active-electron approximation the dipole moment of the HOMO should be used. A better approximation, however, is to use the difference  $\Delta\mu$  between the dipoles of the molecule and the cation [21,22]. In our calculations,  $\Delta\mu = 1.1$  and 0.28 a.u. are used for CO and NO, respectively. These were obtained from the Gaussian quantum chemistry package [36], within the B3LYP hybrid exchange-correlation functional and Dunning's correlation consistent basis set (AUG-cc-pVTZ). We found that the second-order correction term (polarizability) does not contribute much to the ionization potential for both molecules and therefore does not modify the ionization rate significantly. The uncorrected MO-ADK theory calculation predicts that the higher ionization rate occurs when the electric field points from the C atom to the O atom (in agreement with the data). When the Stark correction is introduced, however, the corrected MO-ADK theory calculation favors the opposite direction (in contrast to the data).

Shown in Fig. 11(b) are the results of a SFA calculation, similar to that described by Eq. (12) of Ref. [21]. For this calculation a short two-color (400 and 800 nm in an intensity ratio of 0.09) laser pulse, rather than a dc electric field, was used. The angle between the maximum electric field and a vector pointing from the C atom to the O atom corresponds

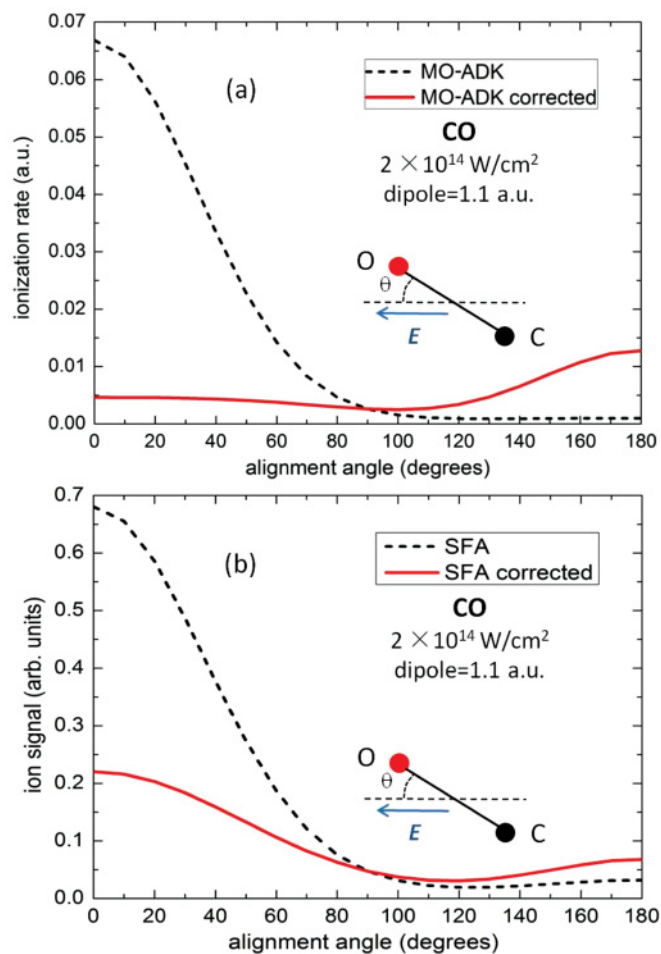


FIG. 11. (Color online) Calculated ionization rates for CO as a function of the angle between the electric field and the molecular axis. The field pointing from C to O corresponds to an angle of  $0^\circ$ . (a) The dashed black curve denotes the MO-ADK theory [5] and the solid red curve denotes the MO-ADK theory corrected for the Stark effect. (b) The dashed black curve denotes the SFA calculation and the solid red curve denotes the SFA calculation corrected for the Stark effect.

to  $0^\circ$ . The results agree qualitatively with the data. In the case of the SFA, the influence of the Stark effect is not sufficient to reverse the trend predicted by the uncorrected SFA and the calculation remains in agreement with the data. A similar conclusion was reached by Etches and Madsen [24] in an analysis of harmonic generation from CO. Figure 12 shows similar calculations for NO. In this case, all of the calculations are in qualitative agreement that the higher ionization rate occurs when the electric field points from the N atom to the O atom, in agreement with the data.

This experiment does not measure explicitly the angular dependences calculated in Figs. 11(b) and 12(b), even though the full time-dependent two-color field was used in the calculations. The reason is that the fragmentation of the molecule requires a second step beyond the removal of the HOMO. Indeed, the generation of dissociative states of the cation, the lower-KER group, may be substantially contaminated by extraction of the HOMO-1 and HOMO-2. Extraction of the HOMO alone from the molecule leaves the molecule in a tightly bound state from which fragmentation will not occur.

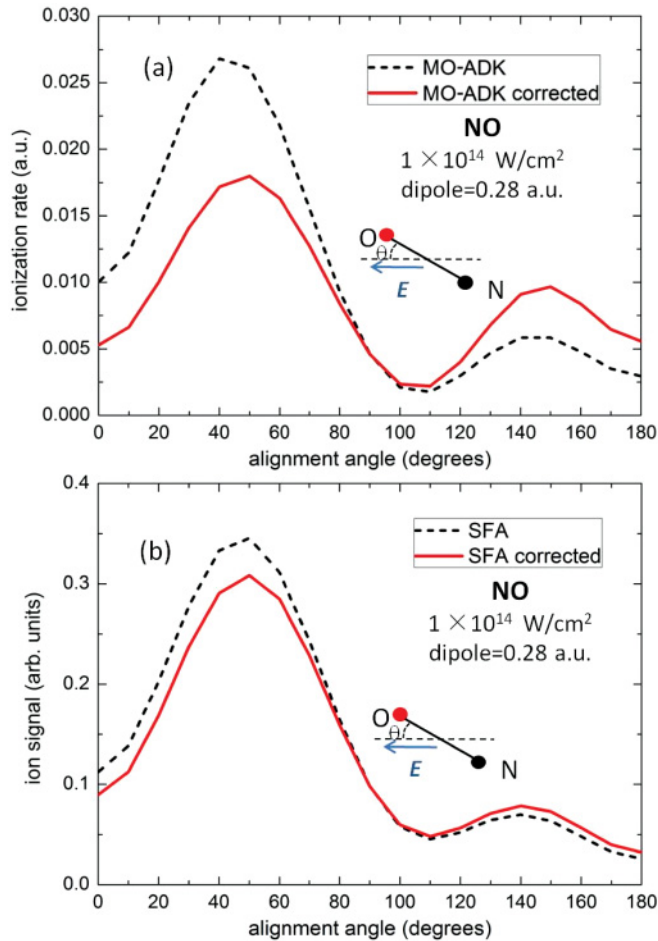


FIG. 12. (Color online) Similar to Fig. 11, but for NO.

A second step, involving rescattering or multiphoton ionization, is required to fragment the molecule, and this process also has an angular distribution. Extraction of the HOMO-1 or HOMO-2, although less likely, can give rise to a highly excited cation from which fragments can be easily produced through bond softening [37]. Thus the use of low-KER fragments to track the angular dependence of the HOMO ionization may not be reliable. For the higher-KER fragments from the dication, at least one HOMO electron is almost certainly removed, but the removal of the second electron, through rescattering, for example, may also have an angular distribution. Only for very low intensities and very short pulses, neither of which was used here, can the influence of this second step be ignored [6–11]. Under the assumption that the angular distribution of the second step were isotropic, one would predict, on the basis of the Stark-corrected SFA results of Figs. 11(b) and 12(b), an asymmetry for  $\phi = 0$  of 0.75 for CO and 0.50 for NO, to be

compared with the experimental values from Figs. 3–5 near 0.30 for CO and from Figs. 4 and 5 near 0.07 for NO. The Stark-corrected SFA predicts correctly the larger asymmetry for CO than for NO. No closer quantitative agreement is obtained or expected.

We point out that the whole situation might be more complicated than a strong-field tunneling approach such as the SFA or MO-ADK theory can handle. While the 800-nm field is in the tunneling region for the intensities used here, the much weaker 400-nm field is not and multiphoton processes involving the second harmonic, involving two or three photons and possible resonant excitations, could possibly play a role in the ionization or fragmentation process. If this is the case, no theoretical treatment short of a full solution of the TDSE including the coupling of many states of the molecules and molecular ions is likely to be fully correct. We do not have such a treatment available to us at present.

Finally we note that in Ref. [18] it is stated that preferential emission of  $C^{2+}$  from CO is in the direction of the electric-field vector. The results presented here are opposite to that, and we have traced this difference to an incorrect assignment of the absolute phase in that part of Ref. [18].

## VI. CONCLUSION

We have established, using a two-color field, that the structure of the HOMO of small heteronuclear molecules is the dominant factor in determining the favored orientation for ionization. We demonstrate this by examining a range of final ions, charge states, and KER. We find that both CO and NO undergo strong-field ionization more readily when the electric field points from C or N toward the O atom. This is in qualitative agreement with the expectations of the MO-ADK theory and with a Stark-corrected version of a SFA calculation. This result can be used to determine the direction of the field in any two-color experiment.

## ACKNOWLEDGMENTS

This work was supported by the Chemical Sciences, Geosciences and Biosciences Division, Office of Basic Energy Sciences, Office of Science, U.S. Department of Energy. W.C. was supported by the National Science Foundation under Grant No. CHE-0822646. G.L. was supported by the U.S. Army Research Office under Grant No. W911NF-07-1-0475. I.Z. and M.F.K. are grateful for support from the DFG via the Emmy-Noether program, the International Collaboration in Chemistry program, and the Cluster of Excellence: Munich Center for Advanced Photonics (MAP). We thank L.B. Madsen, R.R. Jones, I.B. Itzhak, and B. Esry for helpful discussions and H. Ohmura and B. Jochim for sharing data prior to publication.

- [1] M. V. Ammosov, N. B. Delone, and V. P. Krainov, *Zh. Eksp. Teor. Fiz.* **91**, 2008 (1986) [*Sov. Phys. JETP* **64**, 1191 (1986)].  
 [2] L. V. Keldysh, *Zh. Eksp. Teor. Fiz.* **47**, 1945 (1964) [*Sov. Phys. JETP* **20**, 1307 (1965)].  
 [3] F. H. M. Faisal, *J. Phys. B* **6**, L89 (1973).

- [4] H. R. Reiss, *Phys. Rev. A* **22**, 1786 (1980).  
 [5] X. M. Tong, Z. X. Zhao, and C. D. Lin, *Phys. Rev. A* **66**, 033402 (2002).  
 [6] A. S. Alnaser, S. Voss, X.-M. Tong, C. M. Maharjan, P. Ranitovic, B. Ulrich, T. Osipov, B. Shan, Z. Chang, and C. L. Cocke, *Phys. Rev. Lett.* **93**, 113003 (2004).

- [7] A. S. Alnaser, C. M. Maharjan, X.-M. Tong, B. Ulrich, P. Ranitovic, B. Shan, Z. Chang, C. D. Lin, C. L. Cocke, and I. V. Litvinyuk, *Phys. Rev. A* **71**, 031403 (2005).
- [8] S. Voss, A. S. Alnaser, X.-M. Tong, C. Maharjan, P. Ranitovic, B. Ulrich, B. Shan, Z. Chang, C. D. Lin, and C. L. Cocke, *J. Phys. B* **37**, 4239 (2004).
- [9] I. Znakovskaya, P. von den Hoff, S. Zherebtsov, A. Wirth, O. Herrwerth, M. J. J. Vrakking, R. de Vivie-Riedle, and M. F. Kling, *Phys. Rev. Lett.* **103**, 103002 (2009).
- [10] P. von den Hoff, I. Znakovskaya, M. F. Kling, and R. de Vivie-Riedle, *Chem. Phys.* **366**, 139 (2009).
- [11] P. von den Hoff, I. Znakovskaya, S. Zherebtsov, M. F. Kling, and R. de Vivie-Riedle, *Appl. Phys. B* **98**, 659 (2010).
- [12] A. Staudte *et al.*, *Phys. Rev. Lett.* **102**, 033004 (2009).
- [13] H. Akagi, T. Otobe, A. Staudte, A. Shiner, F. Turner, R. Doerner, D. M. Villeneuve, and P. B. Corkum, *Science* **325**, 1364 (2009).
- [14] L. Holmegaard *et al.*, *Nature Phys.* **6**, 428 (2010).
- [15] I. V. Litvinyuk, K. F. Lee, P. W. Dooley, D. M. Rayner, D. M. Villeneuve, and P. B. Corkum, *Phys. Rev. Lett.* **90**, 233003 (2003).
- [16] Pavičić, K. F. Lee, D. M. Rayner, P. B. Corkum, and D. M. Villeneuve, *Phys. Rev. Lett.* **98**, 243001 (2007).
- [17] L. Holmegaard, J. H. Nielsen, I. Nevo, H. Stapelfeldt, F. Filsinger, J. Küpper, and G. Meijer, *Phys. Rev. Lett.* **102**, 023001 (2009).
- [18] S. De *et al.*, *Phys. Rev. Lett.* **103**, 153002 (2009).
- [19] M. Muramatsu, M. Hita, S. Minemoto, and H. Sakai, *Phys. Rev. A* **79**, 011403 (2009).
- [20] I. Znakovskaya, P. Von den Hoff, N. Schirmel, G. Urbasch, S. Zherebtsov, D. Bergues, R. de Vivie-Riedle, K.-M. Weitzel, and M. F. Kling, *Phys. Chem. Chem. Phys.* **13**, 8653 (2011).
- [21] D. Dimitrovski, C. P. J. Martiny, and L. B. Madsen, *Phys. Rev. A* **82**, 053404 (2010).
- [22] Jonas L. Hansen, Henrik Stapelfeldt, Darko Dimitrovski, Mahmoud Abu-samha, Christian P. J. Martiny, and Lars Bojer Madsen, *Phys. Rev. Lett.* **106**, 073001 (2011).
- [23] M. Abu-samha and L. B. Madsen, *Phys. Rev. A* **82**, 043413 (2010).
- [24] A. Etches and L. B. Madsen, *J. Phys. B* **43**, 155602 (2010).
- [25] H. Ohmura, N. Saito, H. Nonaka, and S. Ichimura, *Phys. Rev. A* **77**, 053405 (2008).
- [26] H. Ohmura, N. Saito, and T. Morishita, *Phys. Rev. A* **83**, 063407 (2011).
- [27] K. J. Betsch, D. W. Pinkham, and R. R. Jones, *Phys. Rev. Lett.* **105**, 223002 (2010).
- [28] D. Ray, Z. Chen, S. De, W. Cao, I. V. Litvinyuk, A. T. Le, C. D. Lin, M. F. Kling, and C. L. Cocke, *Phys. Rev. A* **83**, 013410 (2011).
- [29] A. T. J. B. Eppink and D. H. Parker, *Rev. Sci. Instrum.* **68**, 3477 (1997).
- [30] L. Dinu *et al.*, *Rev. Sci. Instrum.* **73**, 4206 (2002).
- [31] M. Vrakking, *Rev. Sci. Instrum.* **72**, 4084 (2001).
- [32] T. Morishita, A.-T. Le, Z. Chen, and C. D. Lin, *Phys. Rev. Lett.* **100**, 013903 (2008).
- [33] M. Lundqvist, P. Baltzer, D. Edvardsson, L. Karlsson, and B. Wannberg, *Phys. Rev. Lett.* **75**, 1058 (1995).
- [34] S. De *et al.*, *Phys. Rev. A* **84**, 043410 (2011).
- [35] A. Zavriyev, P. H. Bucksbaum, H. G. Muller, and D. W. Schumacher, *Phys. Rev. A* **42**, 5500 (1990).
- [36] M. J. Frisch *et al.*, compute code GAUSSIAN 03, revision C.02, Gaussian, Inc., Pittsburgh, PA, 2003.
- [37] H. Akagi, T. Otobe, A. Staudte, A. Shiner, F. Turner, R. Doerner, D. M. Villeneuve, and P. B. Corkum, *Science* **325**, 1364 (2009).